Fourier–Plane Spot Array Generation Using Ion-Exchanged Diffraction Grating : Experimental and Theoretical Study

توليد مصفوفة فورير من النقط المضيئة باستخدام محزز الحيود المصنع بطريقة التبادل الايوني: دراسة نظرية وعملية

Assoc. Prof. A. Shaban Samra

Electronics and Communications Department, Faculty of Engineering, Mansoura University

خلاصة البحث:

في هذا البحث استخدمنا محزز الحيود المصنع بطريقة التبادل الايوني المزدوج في توليد مصفوفة فورير من النقط الضوئية عمليا. ولقد وجد أن نسبة طول المحزز الي عرض شعاع الليزر مهمة في تحديد تصرفات ونتائج هذا المحزز. وباستخدام شعاع ليزر عرضه ٢٠ ميكرومتر وطول موجته هو ٠,٦٣٢٨ ميكرومتر واطوال مختلفة للمحزز امكننا الحصول علي نتائج عملية مختلفة. وقد تم مقارنة هذه النتائج العملية بالأخري النظرية والناتجة عن استخدام طريقة تحويلات فورير للأنتشار الأشعاعي وكان هناك توافق كبير بينهما.

Abstract— In This paper, we have employed a double-ion exchanged diffraction grating, to generate experimentally Fourier spot plane arrays. The grating-length-to-beam-width ratio (d/w_0) is found to be an important parameter in determining device performance. With beam width 20μm (w_0=20μm), center wavelength of λ=0.6328μm, and changing in interaction length (d) and incident angle several basic results are predicted. We compared our results with the numerical solution using fast Fourier transform beam propagation method (FFT-BPM) and there is a good agreement between them.

Key words : grating, diffraction, fast Fourier transform beam propagation method (FFT-BPM).

1. Introduction

Recently, there has been significant progress in the development of two - dimentional arrays of optical and optoelectronic devices. One of the most important technologies for these devices is the SEED (self-electrooptic effect device) technology, which based on multiple quantum-well(MQW) modulator. Multiple quantum wells consist of thin alternating layers of narrow-and wide-bandgap materials such as GaAs and AlGaAs.

The (SEED) technology requires an optical power supply to clock the device. The generation of 2D arrays of uniform intensity spots requires two basic components. The first is a high–power, single frequency, diffraction–limited laser that can provide the appropriate power per pixel required to meet the system speed requirements. The second is some mechanism to equally and uniformly divide the power from the laser and distribute it to the optical windows of the SEEDs[1]. There are several different approaches to the distribution of opical power to SEEDs smart pixels. The approach that has been pursued in the AT&T system demonstrators was Fourier–plane spot array generation using binary phase grating (BFG) to uniformly distributing the optical power to the SEEDs[2-4].

Ion – exchanged glass waveguides have a lot of advantages compared with other waveguide technologies. First, the refractive index of glass can be very close to that of fibers, and a perfect match of the waveguide mode with conventional Single–mode fiber (SMF) is possible. Second, for most optical glasses, the

Accepted June 4, 2007

attenuation due to absorption at telecommunication wavelength is very low. Third, most glasses have negligible birefringence. Finally and most attractive, the ion-exchange process is simple and reproducible [5].

For the above advantages we have fabricated an optical grating by the double ion-exchange technique[6] and used it experimentally to generate Fourier spot plane arrays.

2- Description of grating in terms of the Fourier transform

Fourier transforms is a mathematical operation which relate function in real space to a corresponding set of functions in "reciprocal space". An example of this is the relationship between an object and its Fraunhofer diffraction pattern. Features which are large in real space are small in reciprocal space and vice versa. A multiplication in real space leads to a convolution in reciprocal space and the convolution in real space leads to multiplication in reciprocal space, a shift in real space leads to a change in phase in reciprocal space.

Let us now consider grating within this framework. Our starting point is a "Dirac comb" : a function which consists of an infinite series of delta functions separated by a distance Λ as in Fig.(1), The Fourier transform for this Dirac comb is simply given by [7-9]

$$\sum_{n=-\infty}^{n=0} exp(2\Pi jn \wedge s)$$

where s is the point in the plane of the focused diffraction pattern defined by $(\sin\theta)/\lambda = S$ and θ is the angle of incidence. If we take the terms in pairs corresponding to +n and –n

$$\sum_{n=0}^{n=\infty} exp(2\Pi jn \wedge s) + exp(-2\Pi jn \wedge s) =$$

$$\sum_{n=0}^{n=\infty} 2cos(2\Pi n \wedge s)$$

if (ΛS) is an integer m then the value of $\cos(2\Pi n\Lambda S)$ is unity. If (ΛS) is not an integer then the series sums to zero because for any value of $(2\Pi n\Lambda S)$ later in the series there will be a corresponding value of $(2\Pi n\Lambda S+\Pi)$ which will cancel it.

The Fourier transform of a Dirac comb of spacing Λ is itself a Dirac comb but of spacing $(1/\Lambda)$ since the function is zero everywhere except when $S=m/\Lambda$ or $\Lambda\sin\theta=m\lambda$ which is of course the grating equation for normal incidence and the peaks of the Dirac Comb in the Fourier transform are simply the diffracted orders of the grating.

In practice gratings are not infinite in extent and we may represent this by multiplying the Dirac Comb by a top-hat function, as shown in Fig.2(a).The result of this is that in reciprocal space the Dirac Comb is convoluted with the sinc function ($\sin\beta/\beta$) (where $\beta=\Pi\ \Lambda S$) which is the Fourier transform of the finite aperture, and this is shown in Fig.2(b). Thus we see that in practice the spectral image has a finite width which is inversely proportional to the width of the grating. Again, in practice, gratings do not consist of series of infinitely narrow slits but of grooves of finite width and recognizable profile. The groove profile is then convoluted with the basic Dirac Comb and we would therefore expect that the reciprocal Dirac Comb would be multiplied by the Fourier transform of the groove profile so that the various spikes would have different intensities. We may now regard a diffraction grating as a Dirac Comb multiplied by a top-hat function and convoluted with a groove profile. In the

plane of the focused spectrum we observe, for each wavelength incident upon the grating, its Fourier transform which consists of a Dirac Comb (the orders of diffraction) convoluted with a sinc function (due to the finite width) and multiplied by an envelope function (the blaze effect of the grooves). In real space we have Fig. 3(a) and in reciprocal space, Fig. 3(b).

This description gives us a neat summary of the properties of a grating and demonstrates the way in which the various aspects of a grating affect its performance. The results relating to a perfect grating have already been obtained by other means, but the value of the Fourier transform view of a grating is that it gives us some immediate intuitive insight into the effects of deviations from perfection.

3- Experimental set-up and results

The phase grating used in the present application is made by ion– exchanged technique [6] .This grating is illuminated by a plane wave from a laser source (λ= 0.6328 μm) as illustrated in Fig. 4. The light transmitted through the grating is Fourier transformed at the back focal plane of the lens which is output plane of the spot array generator. Because of the long grating interaction length, the features of the finite beam diffraction are expected to be easily observed in the waveguide geometry. Fig. 5 shows the photographs for diffraction pattern from our grating using laser beam λ= 0.6328 μm with width w_0=20 μm and incident angle on the grating by a Bragg angle (1.2°) at different interaction lengthes (d). Fig.(5-i-a) shows the patterns at d=474 μm ,Fig(5-i-b) at d=600 μm, and Fig.(5-i-c) at d=850 μm. It is clear that at d=474μm the output power is concentrated in one order, by using a cylinderical lens. This pattern changes to a light spot as shown in Fig.(5-ii-a) and by using MATLAB programe this light spot changes to a beam intensity curve as shown in Fig.(5-iii-a). By the same manner the diffraction patterns at d=600μm (where the zero and the first order (± 1) diffraction patterns are observed) and at d=850 μm (where multi-orders diffraction patternsare are observed) are obtained as shown in Fig.(5-i-b,c) as well as their light spots by using cylindrical lens also obtained as shown in Fig.(5-ii-b,c). Finally their beam intensities are obtained by using MATLAB program as in Fig.(5-iii-b,c). From the above curves of Fig.(5) a number of light spots can be obtained by changing the grating interaction length (d).

4- Numerical solution using fast Fourier transform beam propagation method (FFT-BPM).

A beam propagation method (BPM) is a method to simulate the propagation of an optical beam excitation along a waveguide structure. Various kinds of BPMs, such as fast Fourier transformation (FFT-BPM) [10-11] are used.

The BPM is essentially a particular approach for approximating the exact wave equation for monochromatic waves, and for solving the resulting equations numerically. In this section, the basic approach is illustrated by formulating the problem under the restrictions of a scalar field (i.e., neglecting polarization effects) and paraxiality (i.e., propagation restricted to a narrow range of angles). BPM is based on Maxwell's equations [10] and the scalar wave equation for the propagating beam problem is deduced as [11]

$$\frac{\partial^2 u}{\partial z^2} + 2j\beta\frac{\partial u}{\partial z} + \frac{\partial^2 u}{\partial x^2} + \frac{\partial^2 u}{\partial y^2} + (k^2 - \beta^2)u = 0$$

where $k^2 = k_0^2 n^2$, $\beta^2 = k_0^2 n_o^2$ and k is known as the wave- number. In free space, $k_0 = 2\pi/\lambda$. n(x,y) is the refractive index distribution of waveguide structure, and n_o the reference refractive index to be appropriately chosen.

It is now assumed that the variation of u with z is sufficiently slow so that the first term of u above can be neglected with respect to the second; this is the familiar slowly varying envelope approximation, and in this context it is also referred to as the paraxial or parabolic approximation. With this assumption and after slight rearrangement, the above equation reduces to

$$\frac{\partial u}{\partial z} = \frac{j}{2\beta}\left(\frac{\partial^2 u}{\partial x^2} + \frac{\partial^2 u}{\partial y^2} + (k^2 - \beta^2)u\right)$$

This is the basic BPM equation in three dimensions (3-D). Simplification to two dimensions (2-D) is obtained by omitting any dependence on y. Given an input field u (x,y,z=0), the above equation determines the evolution of the field in the space z>0.

In the beam propagation method one propagates an input field u(x,y,z) over a small distance Δz to obtain the field at $z+\Delta z$. The FFT-BPM calculation procedure for a period Δz can be summarized as follows [12], where steps *i-v* correspond to the labels in Fig. (6):

i. At the propagation position z, one calculates the spectral domain wave function $U_{mn}(z)$ in the Fourier transform domain by taking the Fourier transform of the space-domain wave function U(x,y,z).

ii. To get the transformed wave function $U_{mn}(z + \Delta z/2)$ at $z + \Delta z/2$, one multiplies

$$\exp\left(j\frac{(2\pi)^2}{4\beta}\left[\left(\frac{m}{X}\right)^2 + \left(\frac{n}{Y}\right)^2\right]\Delta z\right)$$

by the spectral domain wave function $U_{mn}(z)$ obtained in step *i*. This multiplication corresponds to the propagation over the distance $\Delta z/2$ in free space, where $X = \Delta x.i$,

$0 \le i \le M-1$, $Y = \Delta y.h$, $0 \le h \le N-1$, $X = \Delta x.M$, $-M/2 \le m \le M/2-1$, $Y = \Delta y.N$, $-N/2 \le n \le N/2-1$, X and Y are the widths in the x and y directions.

iii. Taking the inverse Fourier transform of the spectral domain wave function $U_{mn}(z+\Delta z/2)$ obtained in step *ii*, one obtains the space-domain wave function $u(x,y,z+\Delta z/2)$ just in front of the phase-shift lens. Then, multiplying the phase-shift term $\exp(-\chi)$ due to the phase-shift lens by the space - domain wave function $u(x,y,z+\Delta z/2)$, one obtains the space-domain wave function just after the phase-shift lens:

$$\exp(-j\chi)u(x,y,z+\Delta z/2)$$

where

$$\chi = \frac{k_0^2}{2k_0 n_{eff}}\{(n_{eff} + \Delta n)^2 - n_{eff}^2\}\Delta z.$$

iv. Taking the Fourier transform of the space-domain wave function just after the phase-shift lens and multiplying it by

$$\exp\left(j\frac{(2\pi)^2}{4\beta}\left[\left(\frac{m}{X}\right)^2 + \left(\frac{n}{Y}\right)^2\right]\Delta z\right)$$

corresponding to the propagation over $\Delta z/2$ in free space, we obtain the spectral domain wave function $U_{mn}(z + \Delta z)$ at $z + \Delta z$.

v. When the space-domain wave function $u(x, y, z + \Delta z)$ at $z + \Delta z$ is necessary, one must take the inverse Fourier transform of the spectral domain wave function $U_{mn}(z + \Delta z)$ obtained in step *iv* [10].

Repeating steps *i-v*, we can get the space-domain wave function at the target propagation position. It should be noted that if the space-domain wave function at each $z + \Delta z$ is not necessary, one should

return directly to step *ii* from step *iv* and repeat steps *ii-iv*.

The accuracy of the method of course depends on the smallness of the step size Δz and the grid size Δx, Δy, as well as on the size of computation domain.

The numerical simulations are applied to planar diffraction grating waveguide [6]. The measured values of the grating of the effective refractive index of the guided wave mode (n_{e1} and n_{e2}) have been done with a He-Ne laser (λ=0.6328μm) through prism couplers are equal to n_{e1}= 1.512689, n_{e2} = 1.513739, periodicity of the grating is (Λ=10 μm) with incident angle of the optical wavelength as a Bragg angle is given by

$$\theta_B = \sin^{-1}\left[\frac{\lambda}{2n_{e1}\Lambda}\right] \quad \theta_B(\lambda) = 1.1985085^\circ$$

A Gaussian profile whose full width at half maximum is w_o=20 μm is used as the initial field profile $U_o(x_i, z_o) = \exp(-2x_i^2/w_o^2)$. The computational window is 150 μm for the simulation. The accuracy of the results depend on the number of grid points N in the transverse *x* direction, and the size of the propagation steps, Δz in the direction of propagation, z-direction. For N=128, Δz=1 μm the simulation results are shown in Fig. (7-a,b) for a beam intensity at interaction length 474μm. For more details refer to [12].

5- Verification of experimental results by FFT-BPM.

The results of a numerical study and experimental observations of symmetric finite Gaussian beam diffraction by a planar phase grating fabricated by ion-exchange technique are displayed in Figs. (8-a,b,c) . These figures show the comparison between experimental results and theoretical analysis using FFT-BPM of beam intensity at different interaction lengths. We note that there is very good agreements between experimental and theoretical results.

6- Conclusions

Experimental results for a diffractions patterns using He-Ne laser (λ=0.6328μm) of width w_0=20 μm at different interaction lengths and a Bragg angle of incidence for ion-exchanged diffraction grating have been demonstrated. The output patterns are described as a Fourier transform for the incident wavelength when passing across the grating. There is a good agreement between the theoretical analysis using FFT-BPM and the experimental results at the same wavelength and conditions.

The generation of arrays of uniform intensity spots have been obtained from the diffraction patterns using lens and these spots are useful in SEED's technology.

References

[1] J.H.Kim, B.W. Dudley and P.J. Moyer, "Experimental Demonstration of Replicated Multimode Interferometer Power Splitter in Zr-Doped Sol-Gel," J. Lightwave Technol., Vol.24,No.1, PP.612–616, Jan 2006.

[2]Anthony, L. Lentine, and F. A. P.Tooley, "Free-Space Digital Optical Systems", Proc. IEEE. Vol.82 No.11, PP.1632-1649, Nov.1994.

[3] T. Aklyama, K.Inagaki, Y. Mizuguchi, and T.Ohira, "Fourier Optical processing Beam Forming Network using Optical Waveguide Arrays and Lens for Transmission and reception, " IEICE. Trans. Comm. Vol.E84-B, No 9, Sept. 2001, special issue on innovation in antenna and propagation radio systems,

PP.2413-2420. E84-B, No. 9,Sept. 2001.

[4]A. Azana, R. special Slavik, P. Kockaert, L. R. Chen, and S. Larochelle, "Generation of Customized Ultrahigh Repetition Rate Pulse Sequences Using Superimposed Fiber Bragg grating,'' J. Lightwave Technol., Vol.21, No. 6, PP. 1490–1498, June 2003.

[5] J. Zou, F. Zhao and R.T. Chen, ''Mode –Match Ion-Exchanged Glass-Waveguide Bridge for High Performance Dense Wavelength Division Multiplexing,'' J. Lightwave Technol., Vol.23,No.10, PP.2926–2933, Oct.2005.

[6] Gamma. L, Chartier G.H., Samra. A. S. "A novel Technique for Making Grating Demultiplexers in Iintegrated Optics ",J. phys. D: Appl. Phys., vol.23, pp. 1298-1301,printed in UK,1990.

[7] M.C. Hutley, Diffraction Gratings, Academic press 1982.

[8] J. Azana, and M. A. Muried, ''Real-Time Fourier Transformations Performed Simultaneously over Multi Wavelength signals,'' IEEE Photonics Technol. Lett. Vol. 13, No. 1, PP. 55-57,Jan.2001.

[9] D. L. Flannery, and J. L. Horner, ''Fourier Optical Signal Processing,'' Proc. IEEE, Vol. 77, No. 10, PP. 1511-1526, Oct.1989.

[10] K. Kawano, T. Kitoh, Introduction to Optical Waveguide Analysis, pp.165-231,
Ch. 5, John Wiley & Sons, Inc.,2001.

[11]R. Scarmozzino, A. Gopinath, R. Pregla,and S. Helfert, "Numerical Techniques for Modeling Guided-Wave Photonic Devices " IEEE J. *Quan. Elect.* Vol. 6, No. 1, PP. 150-161,Jan.2000.

[12] A. S. Samra and B. B. Yousif, "Beam Propagation Method Based on Fast Fourier Ttransform and Finite Difference Schemes and Its Application to Optical Diffraction Grating," Mansoura Eng. Journal,(MEJ) Vol. 31, No. 1, PP. E67-E81, March. 2006.

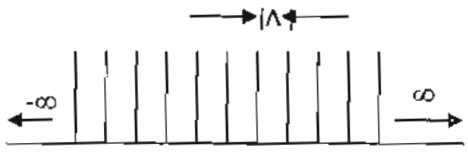

Fig. 1 The "Dirac Comb"

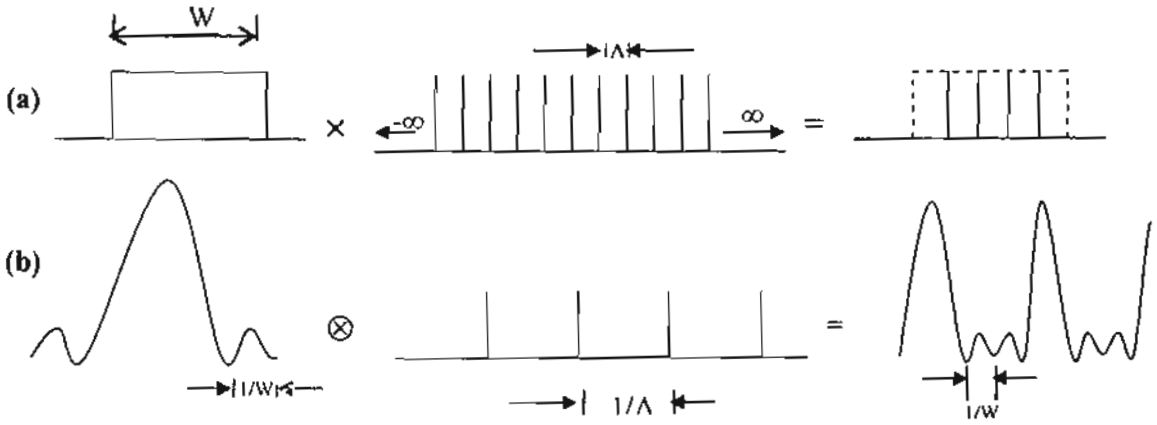

Fig. 2 (a) The gratings are not infinite in extent and represent this by multiplying the Dirac Comb by a top-hat function.

(b) The result of (a) in reciprocal space is the Dirac Comb convoluted with the sinc function which is the Fourier transform of the finite aperture.

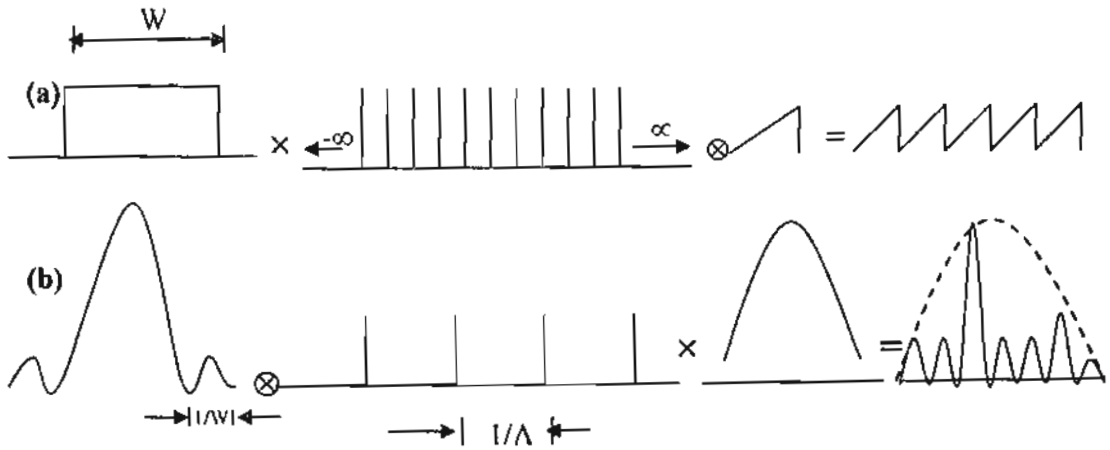

Fig. 3 (a) Representation for grating in real space as Dirac Comb multiplied by a top-hat function and convoluted with a groove profile

(b) Representation for grating in reciprocal space

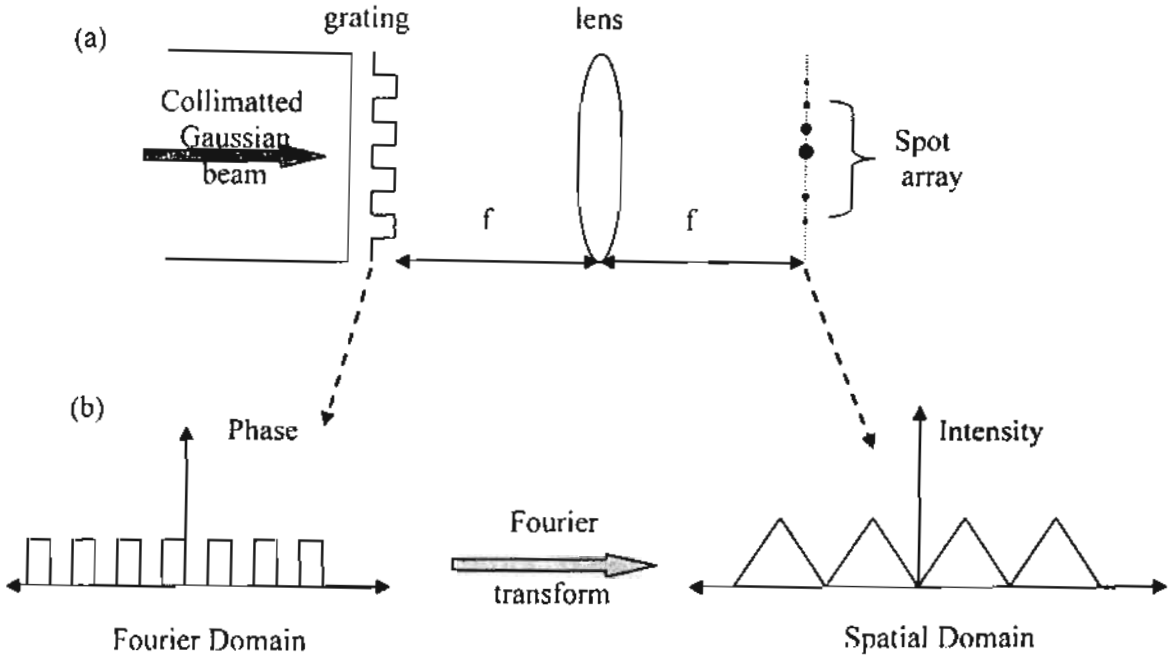

Fig. 4 Fourier-Plane spot array generation

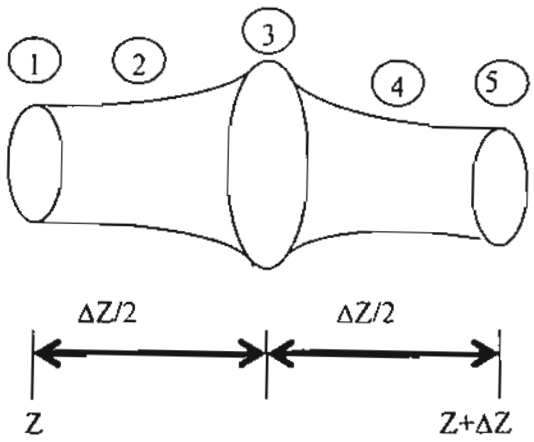

Fig. 6 Calculation of one period in the FFT- BPM.

(a) (b) (c)

(i) diffraction pattern Photographs at different interaction lengths

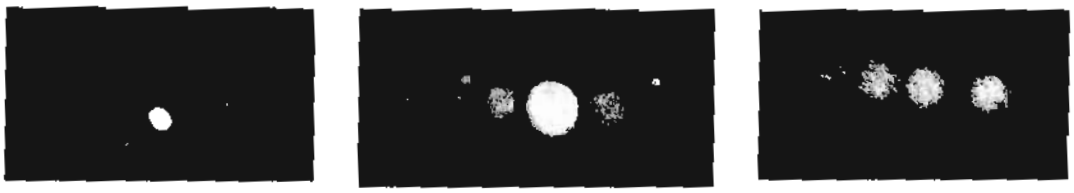

(a) (b) (c)

(ii) light spot photographs for above diffraction patterns

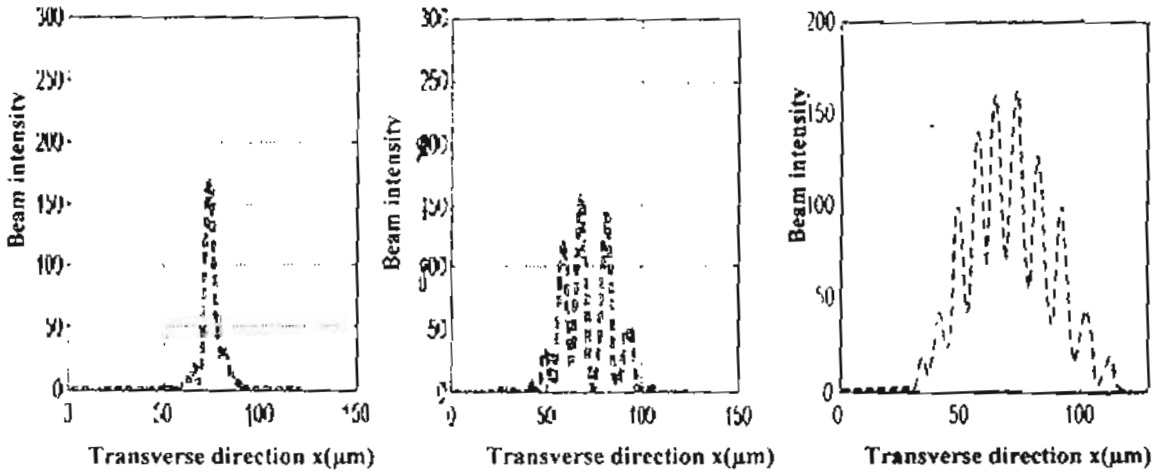

(a) (b) (c)

(iii) light intensities for the diffraction patterns

Fig.5. (i)photographs for diffraction patterns,(ii) light spot photographs for the diffraction Patterns and (iii) light intensities for the diffraction patterns at $\theta_i = 1.2^o$, $W_o = 20$ μm (a) d= 474 μm (b) d = 600 μm (c) d= 850 μm

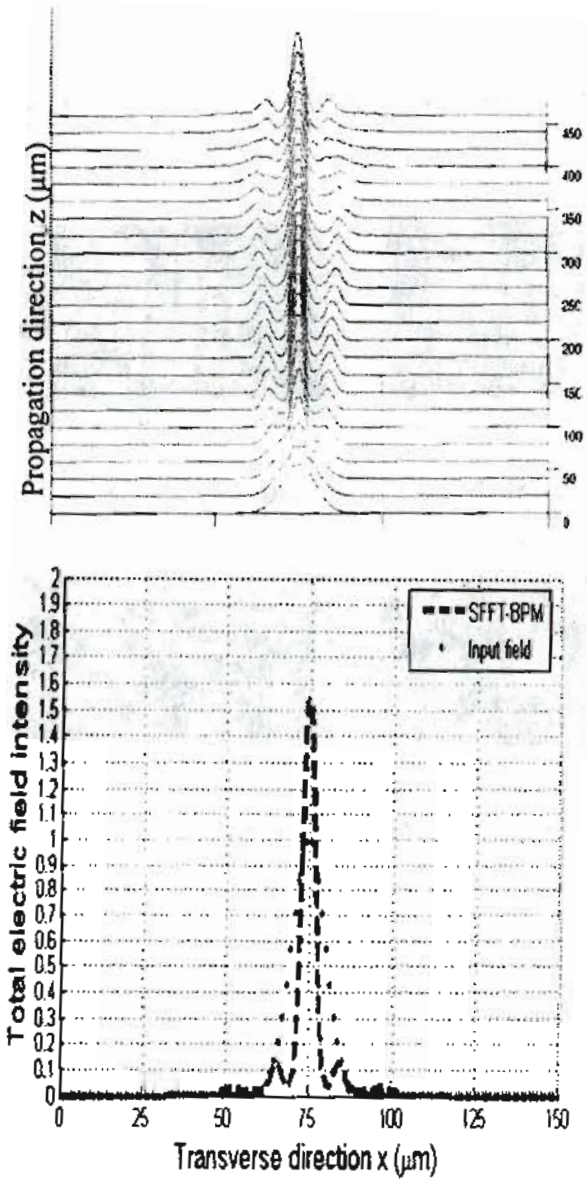

Fig. 7 A grating BPM solution using FFT-BPM
(a)Field profile through 474μm of the grating.
(b) Output beam intensity of 474 μm of the grating.

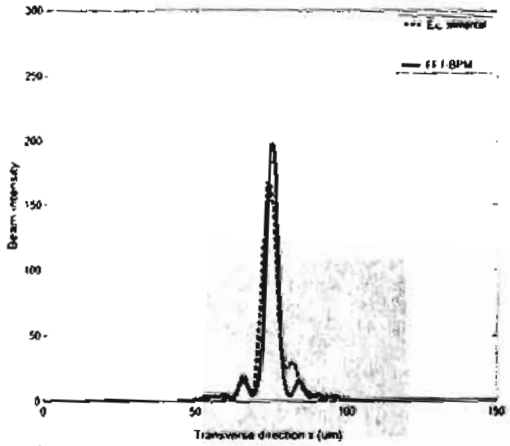

(a)

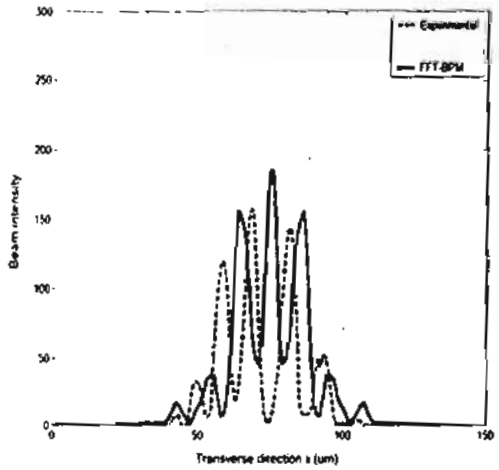

(b)

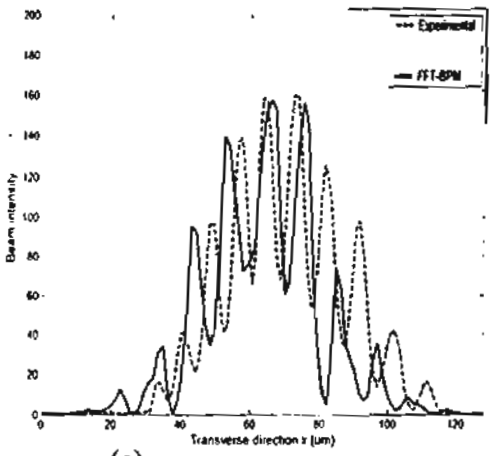

(c)

Fig.8 Comparison between experimental results and theoretical analysis using FFT-BPM of beam intensities at different interaction lengths (a)d=474μm (b)d=600 μm (c)d=850μm.